Combined in-beam electron and γ-ray spectroscopy of ^{184,186}Hg

M. Scheck,[1] P. A. Butler,[1] L. P. Gaffney,[1] N. Bree,[2] R. J. Carrol,[1] D. Cox,[1] T. Grahn,[3] P. T. Greenlees,[3] K. Hauschild,[3,4] A. Herzan,[3] M. Huyse,[2] U. Jakobsson,[3] P. Jones,[3] D. T. Joss,[1] R. Julin,[3] S. Juutinen,[3] S. Ketelhut,[3] R.-D. Herzberg,[1] M. Kowalczyk,[5] A. C. Larsen,[6] M. Leino,[3] A. Lopez-Martens,[3,4] P. Nieminen,[3] R. D. Page,[1] J. Pakarinen,[7] P. Papadakis,[1] P. Peura,[3] P. Rahkila,[3] S. Rinta-Antila,[3] P. Ruotsalainen,[3] M. Sandzelius,[3] J. Saren,[3] C. Scholey,[3] J. Sorri,[3] J. Srebrny,[5] P. Van Duppen,[2] H. V. Watkins,[1] and J.Uusitalo[3]

[1]*Oliver Lodge Laboratory, University of Liverpool, Liverpool L69 7ZE, United Kingdom*
[2]*Instituut voor Kern- en Stralingsfysica, K. U. Leuven, B-3001 Leuven, Belgium*
[3]*Department of Physics, University of Jyväskylä, P.O. Box 35, FI-40014 Jyväskylä, Finland*
[4]*CSNSM, IN2P3-CNRS, F-91405 Orsay Campus, France*
[5]*Heavy Ion Laboratory, University of Warsaw, PL-02097 Warsaw, Poland*
[6]*Department of Physics, University of Oslo, N-0316 Oslo, Norway*
[7]*Physics Department, CERN, CH-1211 Geneva 23, Switzerland*

(Received 21 January 2011; published 29 March 2011)

By exploiting the SAGE spectrometer a simultaneous measurement of conversion electrons and γ rays emitted in the de-excitation of excited levels in the neutron-deficient nuclei ^{184,186}Hg was performed. The light Hg isotopes under investigation were produced using the $4n$ channels of the fusion-evaporation reactions of ^{40}Ar and ^{148,150}Sm. The measured K- and L-conversion electron ratios confirmed the stretched $E2$ nature of several transitions of the yrast bands in ^{184,186}Hg. Additional information on the $E0$ component of the $2_2^+ \rightarrow 2_1^+$ transition in ^{186}Hg was obtained.

DOI: 10.1103/PhysRevC.83.037303 PACS number(s): 21.10.Re, 23.20.Nx, 27.70.+q, 29.30.Dn

Introduction. The neutron midshell Hg and Pb nuclei are some of the most interesting nuclei found in the nuclear landscape. In these nuclei evidence is found that indicates almost degenerate coexisting shapes at low excitation energies [1,2]. For ^{186}Pb, besides the 0^+ ground state the first two excited states are 0^+ states [3]. In the corresponding Hg isotopes, besides the ground-state band, a second band with a bandhead at low excitation energy is observed. Mean-field approaches produce different minima in the potential energy surface [4–7], leading to an identification of these structures as being deformed with one particular macroscopic nuclear shape. In the Pb isotopes these minima are found at deformation values corresponding to spherical, weakly oblate, and prolate shapes. In the light Hg isotopes two distinct minima are associated with weakly oblate and prolate deformation. Based on considerations of the moment of inertia it is proposed that ground-state and low-spin yrast states are members of the weakly oblate deformed band, while the first excited 0^+ state is the bandhead of the well-deformed prolate band. In a simple intruder picture the underlying microscopic proton configurations are a π(0p-2h) two-hole structure (weakly oblate) and a π(2p-4h) two-particle–four-hole structure (prolate) [8], respectively. The bandhead energy of the intruding, prolate π(2p-4h) structure approaches the ground state given by the bandhead of the oblate π(0p-2h) band near neutron midshell at $N = 104$. Furthermore, the energy differences between the individual states of the two bands is lower for the prolate deformed band. Consequently, when approaching midshell the spin of the state for which the prolate band starts forming the yrast band lowers.

The combined spectroscopic study of decay γ rays and electrons offers an opportunity to gain a more detailed picture of the interplay between the oblate and prolate bands. A comparison of the measured intensity ratios for K- and L-conversion electrons allows the transition multipolarities to be determined. Additional $E0$ components in $J_i^\pi \rightarrow J_f^\pi$ ($J_i^\pi = J_f^\pi$) transitions can also be determined quantitatively. The latter is of particular importance for the mixing of states with identical angular momentum belonging to either of the two bands. Various approaches to this problem result in different degrees of mixing [9–12]. In a simple two-level mixing scenario the wave functions of the experimentally observed states $|J_i\rangle$ ($i = 1, 2$) are given as

$$\begin{aligned} |J_1\rangle &= \alpha_1|J_p\rangle + \alpha_2|J_o\rangle|, \\ |J_2\rangle &= -\alpha_2|J_p\rangle + \alpha_1|J_o\rangle, \end{aligned} \tag{1}$$

in the basis of the pure prolate $|J_p\rangle$ and oblate $|J_o\rangle$ states. The monopole strength, $\rho^2(E0)$, is sensitive to the mixing amplitudes, α_n ($n = 1, 2$; $1 = \alpha_1^2 + \alpha_2^2$) (see Eq. (51) in Ref. [13]):

$$\rho^2(E0) = \left(\frac{3}{4\pi}Z\right)^2 \alpha_n^2\left(1-\alpha_n^2\right)\left[\Delta\left(\beta_2^2\right)\right]^2. \tag{2}$$

In Eq. (2) the monopole transition strength, $\rho^2(E0)$, depends on the difference of the deformation parameters β_2 related to the two different shapes of the states connected by the monopole transition. Consequently, the measurement of the $E0$ strength connecting two states with a given J is a very sensitive probe of their mixing.

Experimental considerations. The experiment was conducted at the Accelerator Laboratory of the University of Jyväskylä. The nuclei of interest were produced using the ^{148}Sm(^{40}Ar, $4n$)^{184}Hg* and ^{150}Sm(^{40}Ar, $4n$)^{186}Hg* fusion-evaporation reactions at bombarding energies of 180 and 188 MeV, respectively. To ensure that all electrons were

emitted after the recoiling residue has left the target sample, thin, self-supporting foils of 337 μg/cm^2 (^{148}Sm) and 500 μg/cm^2 (^{150}Sm) thickness were used.

The target area is situated within the new SAGE spectrometer, which has been designed for combined in-beam measurements of electrons and γ rays. A detailed description of SAGE can be found in Ref. [14]. The current setup of the γ-ray detection system of the spectrometer consists of rings 4 ($\Theta = 75.5^{\circ}$), 3 ($\Theta = 104.5^{\circ}$), and 2 ($\Theta = 133.57^{\circ}$) of the JUROGAM HPGe detector array [15]. In this experiment rings 3 and 4 each consisted of 12 four-fold segmented Clover detectors. Ring 2 was equipped with 10 EUROGAM phase-1 detectors. The electron-detection device consists of a solenoid magnet as transportation unit, a high-voltage barrier for the suppression of low-energy δ electrons ($E_{\mathrm{HV}} = -40$ kV), and a 90-fold circular-segmented Si detector. To determine the relative efficiency of the electron-detection device of the spectrometer an open ^{133}Ba source was used. The intensities determined in the spectra were compared with the intensities given in Ref. [16]. The relative efficiency of the γ-ray detectors was determined using ^{133}Ba and ^{152}Eu sources. The observed electron-energy resolution in this preliminary implementation of SAGE was FWHM ≈ 9 keV through the entire energy range.

The program GRAIN [17] was used to construct $\gamma\gamma$ and cross-correlated γe^- matrices from signals observed in coincidence with recoil ions in the GREAT focal plane detector setup [18].

Experimental results for ^{184}*Hg*. A projected electron spectrum of the recoil-gated γe^- matrix for ^{184}Hg is shown in Fig. 1. The experimentally observed electron peak energy, $E_{e^-_{K,L}} = E_\gamma - E_{B,e^-_{K,L}} - E_{\mathrm{Doppler}}$, is shifted by the Doppler energy E_{Doppler} compared to physical energy, given by the difference of the transition energy E_γ and electron binding energy $E_{B,e^-_{K,L}}$ in the K and L shells, respectively. The observed peak structure is attributed to the yrast-band transitions in ^{184}Hg (for a level scheme see Ref. [19]). The energy difference for transitions connecting low-lying yrast states is often similar to the binding-energy difference of 69 keV for electrons

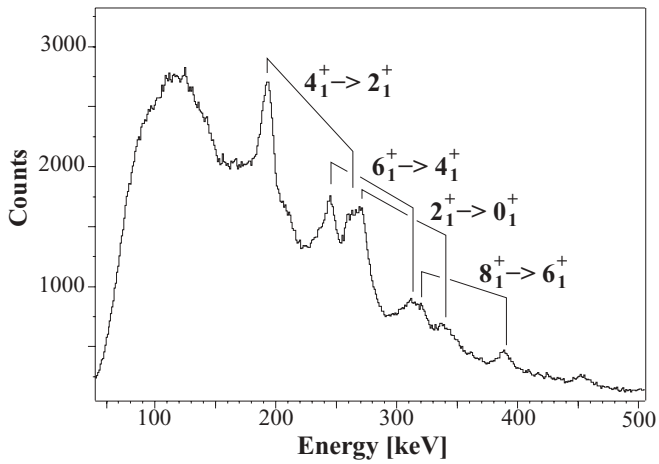

FIG. 1. Projection on the e^- axis of the recoil-gated γe^- matrix of ^{184}Hg. K- and L-conversion electron peaks of one given transition are connected with brackets.

TABLE I. Experimentally observed ratios of K- and L-conversion peaks $(K/L)_{\mathrm{exp}}$ for ^{184}Hg in comparison with tabulated $(\mathrm{K/L})_{\pi L}$ ratios for pure $E2$ and $M1$ multipolarities [20].

$J_i^+ \rightarrow J_f^+$	E_γ (keV)	$(\mathrm{K/L})_{\mathrm{exp}}$	$(\mathrm{K/L})_{E2}$	$(\mathrm{K/L})_{M1}$
$2_1^+ \rightarrow 0_1^+$	366.8	3.4 ± 0.6	2.49(5)	6.02(12)
$4_1^+ \rightarrow 2_1^+$	287.0	1.3 ± 0.2	1.82(4)	5.99(12)
$6_1^+ \rightarrow 4_1^+$	340.1	2.0 ± 0.3	2.27(5)	6.01(12)
$8_1^+ \rightarrow 6_1^+$	418.3	4.4 ± 1.5	2.89(6)	6.04(12)
$10_1^+ \rightarrow 8_1^+$	489.2	2.8 ± 1.2	3.38(7)	6.07(12)

emitted from the K ($E_{B_K} = 83$ keV) and L ($E_{B_L} = 14$ keV) shells [20]. This leads to multiplets in the electron spectrum.

Fusion-evaporation reactions mainly populate yrast states, which allowed the confirmation of the stretched-$E2$ nature of the transitions belonging to the yrast path. The experimentally observed K/L ratios are given in Table I, together with the expected theoretical values. The fitting was done using the total projection of the γe^- matrix on the e^- axis. The theoretical values were calculated with the BRICC data base [20]. Apart from the $8_1^+ \rightarrow 6_1^+$ transition the K/L ratios are within two standard deviations in agreement with K/L ratios of stretched-$E2$ transitions. No evidence for a population of the nonyrast 2_2^+ and 0_2^+ states was found.

Experimental results for ^{186}*Hg*. The lower panel of Fig. 2 shows the electron spectrum for ^{186}Hg (a detailed level scheme is presented in Ref. [21]) obtained by gating on the 187-, 357-, 403-, 405-, 424-, and 489-keV γ-ray peaks of the γe^- matrix. The observed K/L ratios for the transitions of the yrast band are given in Table II. The full projection of the $\gamma\gamma$ matrix is shown in the upper panel. Here, the comparison of intensities of the γ-ray and electron peaks clearly demonstrates that the 216-keV $2_2^+ \rightarrow 2_1^+$ transition must have a strong $E0$ component.

A spectrum created to cross-check the purity of the fit of the $E_{e^-_K} = 124.5$ keV K-shell-conversion electron peak is shown in Fig. 3. In this spectrum the 187.2-keV transition populating the 2_2^+ state and the 405.3-keV transition depopulating the 2_1^+ state are visible. The 402.6-keV $4_1^+ \rightarrow 2_1^+$ transition of the yrast path is not present in the spectrum.

A correlation between the full projection of the $\gamma\gamma$ and γe^- matrices was established. Therefore, for the transitions along the yrast path of ^{184}Hg and ^{186}Hg, the relative efficiency-corrected ratio, $C(\gamma\gamma \leftrightarrow \gamma e^-) = N_{e^-,\mathrm{exp}}/N_{e^-,\mathrm{calc}}$, of measured conversion electrons N_{e^-} and conversion electrons

TABLE II. Experimentally observed ratios of K- and L-conversion peaks $(K/L)_{\mathrm{exp}}$ for ^{186}Hg in comparison with tabulated $(\mathrm{K/L})_{\pi L}$ ratios for pure $E2$ and $M1$ multipolarities [20].

$J_i^+ \rightarrow J_f^+$	E_γ (keV)	$(\mathrm{K/L})_{\mathrm{exp}}$	$(\mathrm{K/L})_{E2}$	$(K/L)_{M1}$
$2_1^+ \rightarrow 0_1^+$	405.3	2.6 ± 1.7	2.77(6)	6.04(12)
$4_1^+ \rightarrow 2_1^+$	402.6	3.0 ± 2.0	2.79(6)	6.04(12)
$6_1^+ \rightarrow 4_1^+$	356.7	2.6 ± 0.9	2.41(5)	6.02(12)
$8_1^+ \rightarrow 6_1^+$	424.2	3.1 ± 1.8	2.93(6)	6.05(12)
$10_1^+ \rightarrow 8_1^+$	488.9	5.1 ± 3.1	3.37(7)	6.07(12)

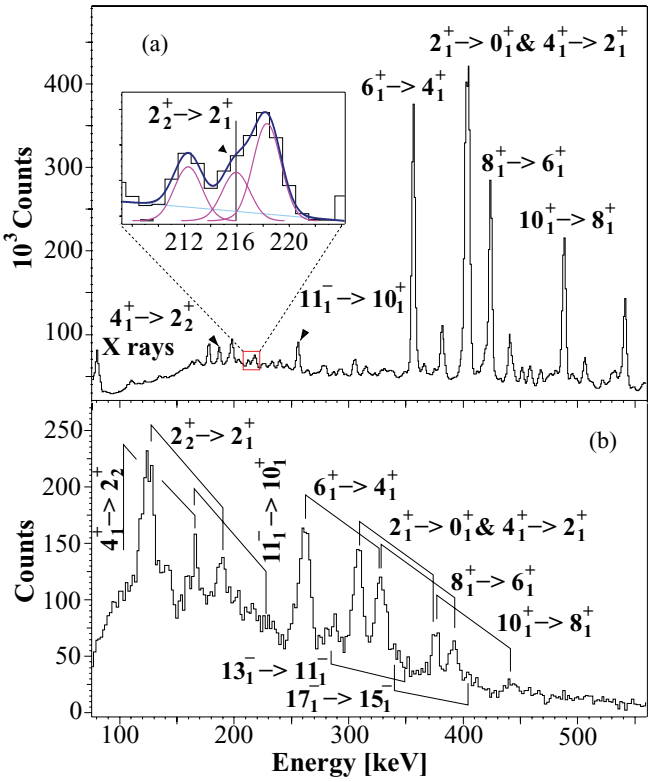

FIG. 2. (Color online) Two spectra of ^{186}Hg simultaneously recorded with the SAGE spectrometer. (a) Projection of the $\gamma\gamma$ matrix. The inset shows the γ-ray peak of the 216-keV $2_2^+ \to 2_1^+$ transition. This peak forms a multiplet with the 212-keV peak (^{185}Au) and the 218-keV peak, the latter stemming from a transition of a K = 8 band [21]. The deconvoluted peaks are shown below the fitted curve. (b) The e^- spectrum created by gating on the 187-, 357-, 403-, 405-, 424-, 489-, and 542-keV γ transitions of the γe^- matrix. K- and L-electron peaks of one given transition are connected with brackets.

expected from the number of γ decays, N_γ,

$$C(\gamma\gamma \leftrightarrow \gamma e^-) = \left(\frac{N_{e^-}}{\epsilon_{\mathrm{rel},e^-}}\right)\left(\frac{W(\Theta, E2)\epsilon_{\mathrm{rel},\gamma}}{\alpha_i(E2)N_\gamma}\right), \qquad (3)$$

was calculated for the individual transitions. The γ-ray angular distribution $W(\Theta, E2)$ for the given setup and transitions was calculated using the efficiency of the JUROGAM phase-1 detectors relative to the efficiency of the Clover detectors. The conversion coefficients $\alpha_i(E2)$ were calculated using the BRICC program [20]. $C(\gamma\gamma \leftrightarrow \gamma e^-)$ was then determined as an error-weighted average of the individual factors. In the present stage of SAGE, it is not possible to obtain any information about the angle at which the electrons were emitted. Hence, an isotropic distribution was assumed.

For the 216-keV $2_2^+ \to 2_1^+$ transition the experimentally observed values for the K- and L-electron to γ-ray emission ratios, $\alpha_i = N_{e^-}/N_\gamma$, were calculated using Eq. (3). The values are given in Table III. Owing to the unknown multipole-mixing ratio, δ, the angular distribution was not considered. For the given setup and assuming that γ rays from the $4^+ \to 2^+ \to 2^+$ and $2^+ \to 2^+ \to 0^+$ cascades contribute to the observed γ-ray peak equally, the angular distributions are calculated as $W(\Theta, M1) = 0.954$ and $W(\Theta, E2) = 1.020$. Consequently,

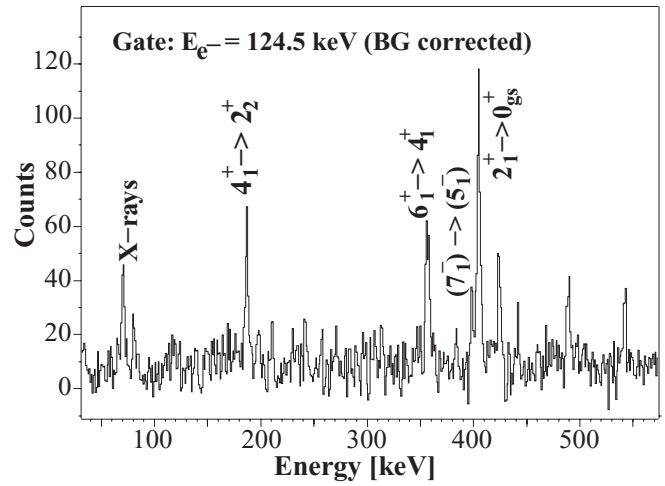

FIG. 3. γ-ray spectrum created by background-corrected gating on the 124.5-keV peak (K-conversion electron peak of the $2_2^+ \to 2_1^+$ 216-keV transition) of the γe^- matrix. The coincident 187- and 405-keV transitions are clearly visible.

5% of the absolute number of observed γ decays has been added to its error.

The intensity ratio $q_K^2(E0/E2) = I_K(E0)/I_K(E2)$ of $E0$- and $E2$-conversion electrons [22] can be expressed as [20]

$$q_K^2\left(\frac{E0}{E2}\right) = \frac{\alpha_K(\mathrm{exp})(1+\delta^2) - \alpha_K(M1) - \alpha_K(E2)\delta^2}{\alpha_K(E2)\delta^2}. \qquad (4)$$

The $q_K^2(E0/E2)$ ratio is dependent on the $E2/M1$ multipole-mixing parameter δ. The $E2$-transition rate $W_\gamma(E2)$ can be calculated from the conversion coefficients and the lifetime $[\tau(2_2^+) = (69 \pm 36)$ ps] [9] of the 2_2^+ state:

$$W_\gamma(E2) = \frac{\delta^2}{(1+\delta^2)[1+\alpha_K(\mathrm{exp})+\alpha_L(\mathrm{exp})]}\frac{1}{\tau}. \qquad (5)$$

However, the experimental monopole strength,

$$\rho^2(E0) = q_K^2\left(\frac{E0}{E2}\right)\frac{\alpha_K(E2)}{\Omega_K(E0)}W_\gamma(E2), \qquad (6)$$

has only a small dependence on the $E2/M1$ multipole-mixing parameter. A variation of the multipole-mixing parameter over a wide range results only in a small variation of the experimental monopole strength [e.g., $\delta = 0,01 : \rho^2(E0) \times 10^3 = 56(47)$, $\delta = 1 : \rho^2(E0) \times 10^3 = 60(50)$, $\delta = 100 : \rho^2(E0) \times 10^3 = 64(52)$]. The large

TABLE III. Experimentally observed K- and L-conversion coefficients, $\alpha_i(\mathrm{exp})$ for the $2_2^+ \to 2_1^+$ transition in ^{186}Hg, in comparison with tabulated values for pure $E2$ and $M1$ multipolarities [20]. Additionally, the electronic factors for $Z = 80$ are given. A detailed discussion is given in the text.

i	$\alpha_i(\mathrm{exp})$	$\alpha_i(E2)$	$\alpha_i(M1)$	Ω_i (1/s)
K	4.9 ± 1.3	0.1417(20)	0.738(11)	1.551×10^{11}
L	1.03 ± 0.26	0.1219(17)	0.1240(18)	2.688×10^{10}

error of the monopole strength arise because of the large error of the lifetime of the 2_2^+ state [9].

In the following the value of $\rho^2(E0) \times 10^3 = 60(50)$ ($\delta = 1$) will be used. This value is of the same order of magnitude as the limit $[\rho^2(E0, 0_2^+ \rightarrow 0_1^+) \times 10^3 > 32]$ observed for the $E0$ transition connecting the bandheads [13]. By exploiting Eqs. (1) and (2), together with the equilibrium quadrupole-deformation parameters $\beta_{\text{oblate}} = -0.15$ and $\beta_{\text{prolate}} = 0.25$ as predicted in Ref. [4], mixing amplitudes of $\alpha_1 = 0.94^{+0.05}_{-0.08}$ and $\alpha_2 = 0.34^{+0.16}_{-0.21}$ are calculated. The corresponding mixing-matrix element is $V_{\text{mix}} = \alpha_1\alpha_2(E_2 - E_1) = 69^{+25}_{-41}$ keV. The bandhead mixing matrix element in ^{186}Hg of $V_{\text{mix}} > 110$ keV [9] is somewhat higher. This finding is astonishing, as for ^{186}Hg the level sequences of the two bands indicate a stronger mixing of the levels with $J = 4$. The level sequence is less disturbed for the 2^+ states and even less for the 0^+ bandheads. For this work, only the strongly mixed wave functions of the 4^+ states allowed for the observation of the $E0$ component in the $2_2^+ \rightarrow 2_1^+$ transitions, as it guarantees a strong enough $4_1^+ \rightarrow 2_2^+$ decay branch $[\text{I}(4_1^+ \rightarrow 2_2^+) = 3.9(4)\%]$ to populate the 2_2^+ state sufficiently.

Acknowledgments. This work has been supported through the Academy of Finland under the Finnish Centre of Excellence Programme 2006–2011 (Nuclear and Accelerator Based Physics Contract No. 213503), the UK Science and Technology Facilities Council, and the European Research Council under the SHESTRUCT project (Grant Agreement No. 203481). The UK/France (STFC/IN2P3) Loan Pool and GAMMAPOOL network are acknowledged. A.C.L. acknowledges financial support from the Department of Physics, University of Oslo, and from the Research Council of Norway (NFR). J.P. has been supported by the European Community's 7th Framework Programme under Contract No. PIEFGA-2008-219175. T.G. acknowledges the support of the Academy of Finland (Project No. 131665).

[1] J. L. Wood, K. Heyde, W. Nazarewicz, M. Huyse, and P. Van Duppen, Phys. Rep. **215**, 101 (1992).
[2] R. Julin, K. Helariutta, and M. Muikku, J. Phys. G **27**, R109 (2001).
[3] A. N. Andreyev *et al.*, Nature (London) **405**, 430 (2000).
[4] S. Frauendorf and V. V. Pashkevich, Phys. Lett. B **55**, 365 (1975).
[5] R. Bengtson and W. Nazarewicz, Z. Phys. A **334**, 269 (1989).
[6] W. Nazarewicz, Phys. Lett. B **305**, 195 (1993).
[7] B. Sabbey, M. Bender, G. F. Bertsch, and P. H. Heenen, Phys. Rev. C **75**, 044305 (2007).
[8] K. Heyde *et al.*, Nucl. Phys. A **466**, 189 (1987).
[9] P. Joshi *et al.*, Int. J. Mod. Phys. E **3**, 757 (1994).
[10] J. Wauters *et al.*, Phys. Rev. C **50**, 2768 (1994).
[11] G. D. Dracoulis, Phys. Rev. C **49**, 3324 (1994).
[12] T. Grahn *et al.*, Phys. Rev. C **80**, 014324 (2009).
[13] J. L. Wood, E. F. Zganjar, C. De Coster, and K. Heyde, Nucl. Phys. A **651**, 323 (1999).
[14] P. Papadakis, AIP Conf. Proc. **1090**, 14 (2009).
[15] [https://www.jyu.fi/fysiikka/en/research/accelerator/nucspec/gamma/jurogam/].
[16] W. H. Trzaska, Nucl. Instrum. Methods A **297**, 223 (1990).
[17] P. Rahkila, Nucl. Instrum. Methods A **595**, 637 (2008).
[18] R. D. Page *et al.*, Nucl. Instrum. Methods B **204**, 634 (2003).
[19] J. K. Deng *et al.*, Phys. Rev. C **52**, 595 (1995).
[20] T. Kibédi *et al.*, Nucl. Instrum. Methods A **589**, 202 (2008).
[21] W. C. Ma *et al.*, Phys. Rev. C **47**, R5 (1993).
[22] E. L. Church, M. E. Rose, and J. Weneser, Phys. Rev. **109**, 1299 (1958).